Investigations on the Reactivity of Bis(bromomagnesio)trimethylsilylmethane – Molecular Structure of a Tebbe-Type Spiro-Organomagnesium Compound

Marijke Hogenbirk,[a,b] Gerrit Schat,[a] Franciscus J. J. de Kanter,[a] Otto S. Akkerman,[a] Friedrich Bickelhaupt,*[a] Huub Kooijman,[c] and Anthony L. Spek[c][‡]

Keywords: Magnesium / Zirconium / Metallocenes / Metallacycles / Structure elucidation

The reactivity of the 1,1-di-Grignard reagent $Me_3SiCH(MgBr)_2$ (**8**) towards transition metal dihalides has been investigated. While most transformations were sluggish and gave no well-defined products, the reaction of **8** with $[Cp_2ZrCl_2]$ in a 1:1 ratio gave, in low yield, the novel spiro-organomagnesium compound $[Cp_2ZrCHSiMe_3(\mu\text{-}Br)]_2Mg$ (**12**), which is stable at room temperature and does not disproportionate on addition of dioxane. An X-ray crystal structure determination has shown that, in the solid state, **12** is present as the C_2 symmetric stereoisomer **12a**; it is sterically very crowded due to the trimethylsilyl substituents. Partial metalla-alkene character is indicated by the short zirconium–carbon bonds, and agostic zirconium–hydrogen interactions by the short zirconium–hydrogen distances (Zr···H–C) and small $^1J_{C,H}$ coupling constants. In benzene solution, equilibrium between **12a** and its C_1 symmetric stereoisomer **12b** was detected by ^1H and ^{13}C NMR spectroscopy.

Introduction

Organometallic reagents carrying two metals at the same carbon atom are often not easily accessible, but they are of interest both because of their intriguing structures and their synthetic applications. A well-known example is Tebbe's reagent (**1**), which is conveniently obtained from titanocene dichloride and trimethylaluminium[1] (Scheme 1); it has found application, for example, in Wittig-type olefinations of ketones.[1,2] We have reported the synthesis of **3**,[3,4] the magnesium analogue of **1**, from bis(bromomagnesio)methane (**2**)[3,5–9] and titanocene dichloride. The chemistry of **2** and of other 1,1-di-Grignard reagents has been reviewed.[10–13]

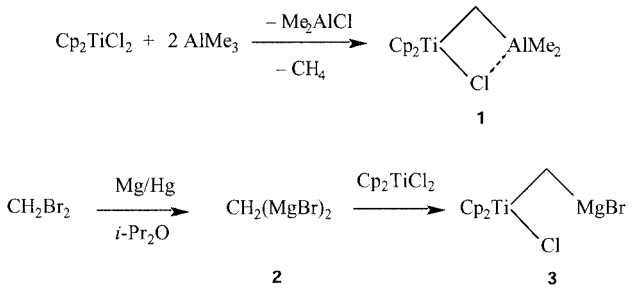

Scheme 1

Like **1** or related 1,1-bismetal-substituted reagents, **3** reacts with alkenes or alkynes to give titanacyclobutanes (**4**) or titanacyclobutenes (**5**), respectively (Scheme 2).[3] Reaction with trimethylphosphane yields the carbene complex **6**.[14] Of special interest here is the elimination of magnesium halide from **3** by evaporation of an ethereal solution followed by dissolution in toluene, which gave, based on its analytical data, $MgBr_2(CH_2TiCp_2)_2$ which was tentatively formulated as the spiro-organomagnesium compound **7**.[4]

Few known derivatives of **2** carry additional substituents at the carbon atom. We previously prepared the mono- and bis(trimethylsilyl)-substituted derivatives **8**[15] and **9**,[16] respectively (Scheme 3). However, silyl substitution stabilizes these di-Grignard reagents considerably. In particular, **9** was extremely sluggish to react even with benzophenone, and attempted reactions with metal dihalides were unproductive. The low reactivity was ascribed both to steric protection and to electronic stabilization of the negatively charged central carbon atom by silicon.[15,16]

Not surprisingly, the reactivity of **8** was intermediate between those of **2** and **9**. Thus, **8** did react with chlorotrimethylstannane; with benzophenone, it gave the expected Wittig-type product 1,1-diphenyl-2-trimethylsilylethene.[15]

[‡] Correspondence concerning the crystallography should be addressed to this author.
[a] Scheikundig Laboratorium, Vrije Universiteit, De Boelelaan 1083, 1083 HV Amsterdam, The Netherlands
Fax: (internat.) + 31-20-4447488
E-mail: bickelhpt@few.vu.nl
[b] Present address: Akzo Nobel, N.V. Organon, Molenstraat 110, P. O. Box 20, 5340 BH Oss, The Netherlands
[c] Bijvoet Center for Biomolecular Research, Utrecht University, Padualaan 8, 3584 CH Utrecht, The Netherlands

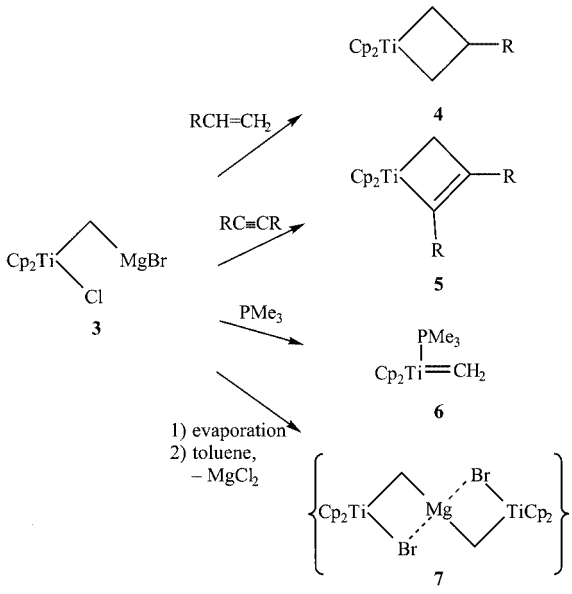

Scheme 2

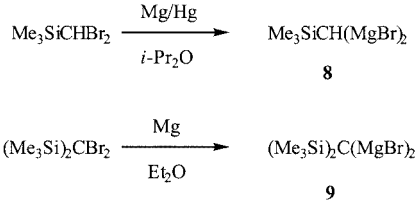

Scheme 3

Thus, we have investigated possible applications of **8**, analogous to those depicted in Schemes 1 and 2, to access the corresponding trimethylsilyl-substituted derivatives.

Results and Discussion

Reactions of $Me_3SiCH(MgBr)_2$ (8)

In analogy to the preparation of 1,3-dimetallacyclobutanes from **2**,[3,10–13] one of our main goals was the reaction of a group 4 metallocene dichloride [Cp_2MCl_2] (M = Ti, Zr, Hf) with **8** in a ratio of 1:2 to obtain the formal 1,3-di-Grignard reagent **10** which was then to be converted with the same (or a different) metal dichloride into the desired 1,3-dimetallacyclobutane **11** (Scheme 4). However, despite considerable efforts, including variation of solvents, reaction conditions etc., complicated reaction mixtures were obtained; even attempted interception of **10** with chlorotrimethylgermane did not furnish clear-cut results.

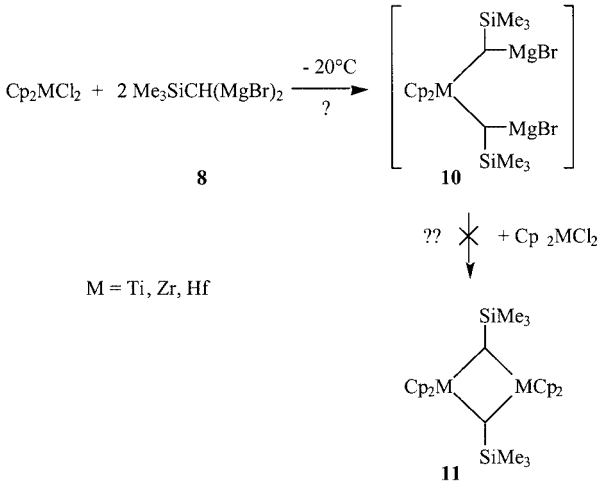

Scheme 4

In contrast, the reaction of [Cp_2ZrCl_2] with **8** in a 1:1 ratio gave an unforeseen product; after workup and purification, **12** was isolated by crystallization from a saturated toluene solution upon standing at room temperature for several weeks. The yield was low; the ^1H NMR spectrum of the crude product revealed several other compounds that could not be identified. A possible reaction pathway via the "Tebbe-type" reagent **13** is depicted in Scheme 5.

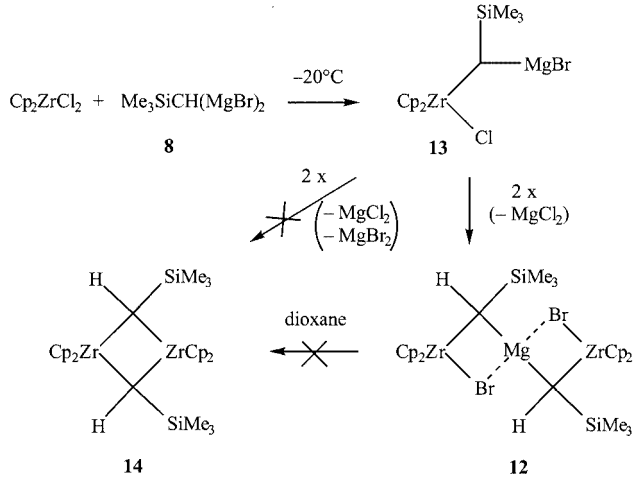

Scheme 5

Although there is no direct evidence for the occurrence of **13**, we assume it is formed by substitution of one of the chlorides of zirconocene dichloride by one of the two organomagnesium functions of **8**. Possibly, in the process of evaporating the reaction mixture and extracting the residue with toluene, **13** undergoes a partial "Schlenk equilibrium" by elimination of $MgCl_2$. Remarkably, the expected second Schlenk equilibrium step under elimination of $MgBr_2$ to furnish the 1,3-dizirconacyclobutane **14** does not proceed, neither from **13** nor from **12**. The latter reaction was tried separately by addition of dioxane to a solution of previously isolated **12**; however, **12** remained unchanged.

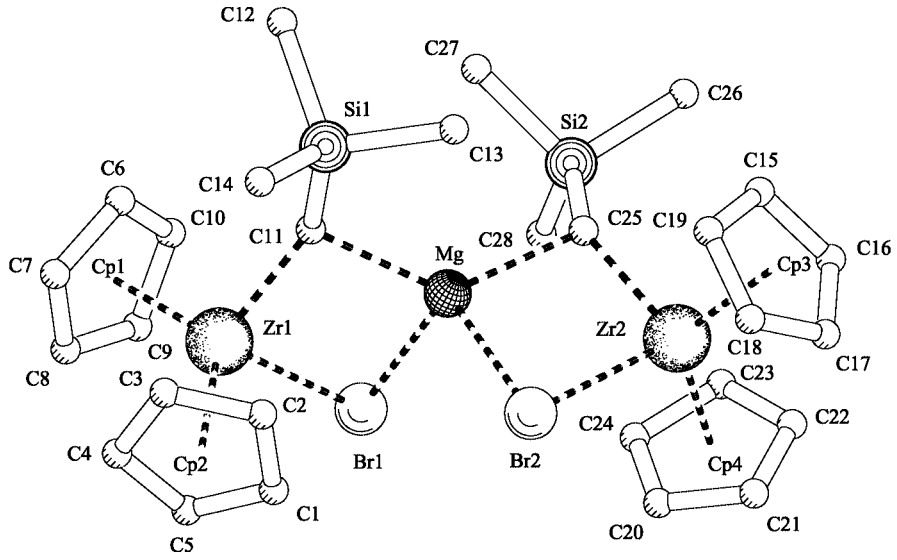

Figure 1. PLUTON[29] drawing of **12**; hydrogen atoms have been excluded for clarity; Cp indicates the center of a five-membered ring

Molecular Structure of $[Cp_2ZrCHSiMe_3(\mu\text{-}Br)]_2Mg$ (12) in the Crystal

From a saturated solution of **12** in toluene, crystals were obtained after standing for two months at room temperature. The pale yellow-orange rectangular crystals were collected and transferred to Lindemann-glass capillaries under a nitrogen atmosphere; the capillaries were then sealed by melting off. The X-ray crystal structure was determined (Figure 1). Selected bond lengths, nonbonded contacts, bond angles, and torsion angles are presented in Table 1−4, respectively.

Table 1. Selected bond lengths of **12**

[a]	Bond length [Å]		Bond length [Å]
Zr(1)−Cp(1)[a]	2.227(4)	Mg−Br(1)	2.672(3)
Zr(1)−Cp(2)[a]	2.239(4)	Mg−Br(2)	2.626(3)
Zr(2)−Cp(3)[a]	2.236(5)	Mg−C(11)	2.188(8)
Zr(2)−Cp(4)[a]	2.222(5)	Mg−C(25)	2.188(8)
Zr(1)−Br(1)	2.7232(11)	Si(1)−C(11)	1.851(8)
Zr(2)−Br(2)	2.7236(11)	Si(2)−C(25)	1.837(8)
Zr(1)−C(11)	2.147(7)		
Zr(2)−C(25)	2.160(7)		

[a] Cp(centroid).

Table 2. Selected nonbonded contacts of **12**

Contact	D(A−B)[a] [Å]	Σ(A−B)[b]	Δ[c] [Å]
Zr(1)···Si(1)	3.779(2)	4.46	−0.68
Zr(2)···Si(2)	3.740(3)	4.46	−0.72
Zr(1)···H(111)	2.496(7)	3.56	−1.06
Zr(2)···H(251)	2.546(7)	3.56	−1.01
C(6)···H(111)	2.722(11)	2.90	−0.18
C(15)···H(251)	2.721(13)	2.90	−0.18

[a] D(A−B) = measured distance between A and B. [b] Σ(A−B) = sum of radii of A and B; contact radii according to: A. Bondi, *J. Phys. Chem.* **1964**, *68*, 441, or covalent radii +0.8 Å. [c] Δ = D − Σ.

Table 3. Selected bond angles of **12**

Bond angle	[°]	Bond angle	[°]
Br(1)−Zr(1)−C(11)	91.7(2)	Zr(1)−C(11)−H(111)	99.1(6)
Zr(1)−C(11)−Mg	97.0(3)	Zr(1)−C(11)−Si(1)	141.8(4)
Zr(1)−Br(1)−Mg	73.99(6)	Si(1)−C(11)−H(111)	101.7(7)
C(11)−Mg−Br(1)	92.2(2)	Si(1)−C(11)−Mg	112.0(4)
Zr(2)−C(25)−Mg	97.0(3)	H(111)−C(11)−Mg	96.4(7)
Zr(2)−Br(2)−Mg	74.96(7)	Si(2)−C(25)−H(251)	105.5(7)
C(25)−Mg−Br(2)	93.9 (2)	Si(2)−C(25)−Mg	112.6(4)
Zr(1)−Mg−Zr(2)	157.09(9)	H(251)−C(25)−Mg	91.2(6)
Br(1)−Mg−Br(2)	103.80(9)	C(11)−Mg−Br(1)	92.2(2)
C(11)−Mg−C(25)	132.6(3)	C(11)−Mg−Br(2)	117.5(2)
Cp(1)··Zr(1)··Cp(2)	129.48(16)	Zr(2)−C(25)−Si(2)	138.6(4)
Cp(3)··Zr(1)··Cp(4)	128.76(19)		

Although the distances and angles in the two four-membered 1,3-metallacycles that constitute **12** are not equal, the compound has nearly C_2-symmetry. The "C_2"-axis passes through magnesium, perpendicular to the Zr(1)−Zr(2) vector, bisecting the Br−Mg−Br angle. As discussed below, in solution, **12** occurs as two equilibrating stereoisomers, **12a** and **12b**. Presumably, **12a** corresponds to the crystal structure, the only difference being that it *does* possess perfect C_2-symmetry, presumably due to time averaging.

Complex **12** is solvent-free, so the magnesium atom is not stabilized by coordinating diethyl ether molecules! This situation is unknown for monomeric organomagnesium compounds; rather, unsolvated organomagnesium compounds tend to crystallize in the form of polymeric ladder-type structures.[17,18] Nevertheless, the magnesium does show the usual tetracoordination with two carbon atoms and two bromine atoms forming the coordination sphere. The geometry around magnesium is distorted tetrahedral, the smallest angle being C−Mg−Br in the four-membered

Table 4. Selected torsion angles of **12**

Torsion angle	[°]	Torsion angle	[°]
Zr(1)−Br(1)−Mg−C(11)	−15.3(2)	Zr(2)−Br(2)−Mg−C(25)	−10.4(2)
Zr(1)−C(11)−Mg−Br(1)	18.9(2)	Zr(2)−C(25)−Mg−Br(2)	12.8(2)
C(11)−Zr(1)−Br(1)−Mg	15.6(2)	C(25)−Zr(2)−Br(2)−Mg	10.5(2)
Si(1)−C(11)−Mg−Br(1)	173.5(3)	Si(2)−C(25)−Mg−Br(2)	163.2(3)
Si(1)−C(11)−Zr(1)−Br(1)	−158.6(6)	Si(2)−C(25)−Zr(2)−Br(2)	−148.8(6)
Mg−C(11)−Zr(1)−Br(1)	−18.5(2)	Mg−C(25)−Zr(2)−Br(2)	−12.3(2)
H(111)−C(11)−Zr(1)−Br(1)	79.1(6)	H(251)−C(25)−Zr(2)−Br(2)	80.4(7)
H(111)−C(11)−Mg−Br(1)	−81.1(6)	H(251)−C(25)−Mg−Br(2)	−89.2(6)
Zr(1)−Br(1)−Mg−Br(2)	103.69(8)	Zr(2)−Br(2)−Mg−Br(1)	106.64(8)
Zr(1)−C(11)−Mg−Br(2)	−87.9(3)	Zr(2)−C(25)−Mg−Br(1)	−94.4(2)
Zr(1)−Br(1)−Mg−C(25)	−155.2(2)	Zr(2)−Br(2)−Mg−C(11)	−153.5(2)
Zr(1)−C(11)−Mg−C(25)	146.6(3)	Zr(2)−C(25)−Mg−C(11)	146.4(3)
Si(1)−C(11)−Mg−Br(2)	66.7(4)	Si(2)−C(25)−Mg−Br(1)	56.0(4)
Si(1)−C(11)−Mg−C(25)	−58.8(5)	Si(2)−C(25)−Mg−C(11)	−63.2(5)

rings [92.2(2) and 93.9(2)], the largest one C(11)−Mg−C(25) (132.6°).

Crowding due to the trimethylsilyl substituents at the methine carbon atoms in combination with the cyclopentadienyl ligands at the zirconium atoms appears to be a prominent feature in the structure of **12**. The *trans*-orientation of the trimethylsilyl substituents reduces the crowding. They stick in between the neighboring cyclopentadienyl rings such that they minimize close contacts with these ligands. In addition, the Zr−C−Si angles are very large (average 140°). As a result, the silicon−carbon bonds form relatively small angles with the average planes of their metallacycle, as evidenced by the torsion angles Si(1)−C(11)−Mg−Br(1), Si(1)−C(11)−Zr(1)−Br(1), Si(2)−C(25)−Mg−Br(2), and Si(2)−C(25)−Zr(2)−Br(2) of 173.5(3)°, −158.6(6)°, 163.2(3)°, and −148.8(6)°, respectively; consequently, the trimethylsilyl substituents are close to the (approximate!) plane of the four-membered rings to which they are attached. However, the close Zr−Si contacts of 3.76 Å (Table 2, mean value) indicate that a really favorable orientation is not achieved as the sum of their contact radii is 4.46 Å. Due to this steric repulsion, the cyclopentadienyl groups are not bonded symmetrically to the zirconium atoms; the Zr−C(Cp) distances range from 2.48 to 2.56 Å.

Apparently, the sterically demanding trimethylsilyl groups also influence the geometry of the two four-membered rings. Firstly, these rings are not planar, as evidenced by the torsion angles Zr(1)−Br(1)−Mg−C(11) of −15.3(2)° and Zr(2)−Br(2)−Mg−C(25) of −10.4(2)°; in contrast, the four-membered ring is planar in the neopentyl-substituted Tebbe reagent $Cp_2ZrCH(CH_2CMe_3)AlCl$[19] (i.e. the zirconium derivative of **1**, in which the methylene group is substituted by the sterically *even more demanding* neopentyl group). Secondly, the two rings are not oriented orthogonally with respect to each other, as indicated by the angle of 85.53(17°) between their average planes. Finally, the axes of these average planes are bent towards each other, the Zr−Mg−Zr angle being 157.09(9)°. Despite these strong steric interactions **12** is, remarkably, thermally quite stable.

In addition to its rather unique spiro-Tebbe character, a closer analysis of the data for **12** reveals an intriguing duality of structural features. At first sight, **12** might be described as a dialkylmagnesium compound. This is in line with the seemingly normal Mg−C bond lengths of 2.188(8)Å, the usual range being 2.17−2.19Å.[17,18] In addition, the wide C−Mg−C angle of 132.6(3)° falls within the normal range (120−140°). Bonds to more electronegative ligands such as oxygen are smaller than tetrahedral; here, the negative ligand is bromine, and the Br−Mg−Br angle of 103.80(9)° fits into the general trend.

However, the Zr−C bonds [2.147(7) and 2.160(7)Å] are ca. 0.15 Å shorter than those in related compounds with "normal" σ-bonds between zirconium(IV) and sp^3-hybridized carbon atoms {[$Cp_2ZrMeCl$]: 2.35 and 2.36 Å;[20] [Cp_2ZrMe_2]: 2.280(5) and 2.273(5) Å;[20] [$Cp_2Zr\{CH(SiMe_3)_2\}Ph$]: 2.329(6)[21]}. Even the Zr−C bond in [$Cp_2Zr(\mu\text{-}\eta^1,\eta^2\text{-}Me_3SiCCPh)(\mu\text{-}Cl)AlMe_2$], in which an sp^2-hybridized carbon is σ-bonded to zirconium, is slightly longer [2.186 (3) Å].[22] The repulsion between the trimethylsilyl groups and the cyclopentadienyl ligands would be expected to lengthen the Zr−C bond.[21] We explain these short Zr−C bonds by invoking a certain amount of metalla-alkene character. A partial double bond will shift the hybridization of carbon from sp^3 towards sp^2 with concomitant bond shortening; in addition, the bond may be shortened by hyperconjugative interactions with silicon.[16] In addition, the Zr−C−Si angle will increase and so create more space for the trimethylsilyl groups; indeed, the Zr−C−Si angle is large [141.8(4)° and 138.6(4)°]. Conversely, the Zr−Br bond lengths are long (Zr1−Br1: 2.7232(11)Å, Zr2−Br2: 2.7236(11)Å]; most Zr−Br bonds are about 2.60 Å. We found only one other example of a long Zr−Br bond involving tetracoordinate zirconium: [$Cp_2ZrBr\{C(SiMe_3)=CHPh)\}$][23] [2.721(1) Å]. All this structural information suggests a description in terms of a loose complex **12′** between [$Cp_2Zr=CHSiMe_3$] and $MgBr_2$ (Scheme 6).

However, the situation is not so clear cut. The metalla-alkene/Lewis-acid character in "Tebbe-type" reagents such as **1**, involving titanium and zirconium in combination with

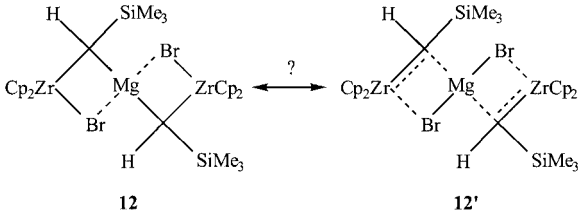

Scheme 6

aluminium, has been discussed on the basis of NMR spectroscopic data, reactivity patterns, and theoretical calculations.[19,25–27] The general conclusion is that the metal–carbene character is not very pronounced for titanium and even less so for zirconium.

As indicated above, the Mg–C bond lengths of 2.188(8) Å seems to fit better with **12** as a dialkylmagnesium.[17,18] For a loose interaction as in **12′**, the bond would be expected to be even longer, and this effect should be enhanced by steric congestion. However, these observations may be interpreted differently by looking at the structure of **9** $[(MeSi_3)_2C(MgBr{\cdot}2THF)_2]$[16] which has rather short Mg–C bonds (2.10–2.14 Å), even though two large trimethylsilyl groups and two large MgBr·2THF functions exert considerable steric pressure around the central carbon. Electrostatic effects which find their origin in the substitution of carbon by four electropositive elements (2 magnesiums, 2 silicons) have been invoked to explain the short Mg–C bonds in **9**.[16] With **12′**, similar factors might play a role, though to a lesser extent: the inherently loose interaction between magnesium and carbon is partly stabilized by polarizing effects due to zirconium and silicon. Conversely, the chemical shift of the bridging carbon in the four-membered ring, $\delta(^{13}C)$ = 153.7 ppm, is not indicative of strong metalla-alkene character, which is usually concomitant with a much more deshielded shift, as illustrated by the Ti=*C*H_2 carbon in **6** with $\delta(^{13}C)$ = 285.2 ppm.[14] The slightly elongated Mg–Br bonds (average 2.65 Å) are compatible with both **12** (μ-bridging between two metals)[17,18] and **12′** (loose interaction of $[Cp_2Zr{=}CHSiMe_3]$ with the Lewis acid $MgBr_2$).

A thorough theoretical analysis is clearly required, which was beyond the scope of the present investigation. From of the qualitative arguments discussed here, we propose that the structure of the compound is intermediate between the two extreme models, which is indicated by the resonance relation depicted in Scheme 6; apparently, **12** is preponderant, but contributions from **12′** are clearly indicated.

Another aspect to discuss briefly is a weak agostic interaction[24,25] between zirconium and the α-CH bond; **12** has short M···H distances and small $^1J_{C,H}$ coupling constants, both of which are characteristic of M···H–C agostic interactions. The Zr···H distances [2.496(7) and 2.546(7) Å] are more than 1 Å shorter than the sum of their contact radii, and $^1J_{C,H}$ = 91.4 Hz is small, though in the upper range for sp^3-hybridized agostic systems (60–90 Hz).

However, two caveats seem appropriate. First, the positions of the α-hydrogens – as light atoms next to the heavy zirconium – were restrained during refinement. Although the C–H moiety as a whole was allowed to reorient itself, the C–H bond was fixed at the ideal value of 0.98 Å. This makes the position of these hydrogens slightly less reliable. Typical β-agostic contacts are shorter, as exemplified by *d*(Zr···H) = 2.19 Å in $[Cp_2ZrBr(CSiMe_3{=}CHPh)]$.[23] Even so, the Zr···H contacts in **12** indicate a weak agostic interaction. Secondly, with regard to the small $^1J_{C,H}$ = 91.4 Hz, one has to consider that substitution of an sp^3-hybridized carbon by electropositive elements increases the s-character in the C–M bonds, and thus reduces s-contribution to the C–H bonds. For instance, we observed $^1J_{C,H}$ = 104.4 Hz for the joint effect of magnesium and silicon in Me_3Si-CH_2MgBr, while the additional silicon in $(Me_3Si)_2$-CHMgBr (**8**) further decreases $^1J_{C,H}$ to 93.1 Hz. However, against this background, it is unlikely that the small $^1J_{C,H}$ = 91.4 Hz of **12** can be fully accounted for by the effect of only three electropositive substituents on carbon (Mg, Zr, Si).

Finally, the X-ray crystal structure of **12** supports the previously suggested hypothetical assignment[4] of an analogous spiro-magnesium structure to **7** (Scheme 2).

Structure of 12 in Solution

Crystals of **12** dissolved in C_6D_6 for NMR analysis showed two species, **12a** and **12b**, in equilibrium; directly after dissolution, **12a** was the dominant species. Its simple ^{1}H NMR spectrum is indicative of C_2 symmetry: δ = 7.43 (s, 2 H, C*H*), 6.09 (s, 10 H, Cp), 5.94 (s, 10 H, Cp), 0.43 (s, 18 H, $SiMe_3$) ppm. Such a spectrum is also in line with the C_2 symmetric structure **12c** (Scheme 7). The immediate appearance of this spectrum after dissolving crystals of **12**, which have been proven to have the (approximate) C_2 structure (Figure 1), strongly suggests that the species in solution is **12a**; its ideal C_2 symmetry must be due to rapid time averaging. This structure assignment is further supported by inspection of models that reveal that the alternative conceivable C_2 isomer **12c** would experience severe steric hindrance because it has two trimethylsilyl groups at the two four-membered rings that point directly towards each other.

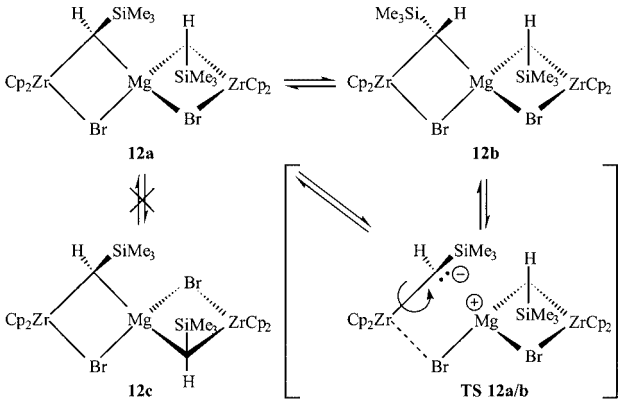

Scheme 7

Compound **12b** is, apparently, an isomer of **12a**, but it has C_1 symmetry, as evidenced by two methine proton signals [δ = 7.80 and 7.17 ppm (2 s, 2 H)], four cyclopentadienyl signals at δ = 6.14, 6.04, 5.95 and 5.94 ppm (4 s, 20 H) and two trimethylsilyl signals at δ = 0.43 and 0.40 ppm (2 s, 18 H). The isomeric relation is in line with the chemical shifts of **12b** all being in the same range as the corresponding signals of **12a**; moreover, **12b** must contain a $MgBr_2$ unit because this species could not be removed from the solution on treatment with THF or dioxane, and free $MgBr_2$ would have precipitated in C_6D_6.

As mentioned above, crystals of **12**, when dissolved in C_6D_6, formed a mixture of **12a** and **12b** where the initial concentration of **12b** was very low. After standing for several days at room temperature, an equilibrium ratio of **12a/12b** = 1.14 was reached. At higher temperatures, the amount of **12a** increased (Table 5); this change was reversible. Below room temperature, the composition of the mixture showed no further changes; apparently, the rate of isomerization was too low.

Table 5. Equilibrium constants and equilibration times of **12a/b** in C_6D_6

T (K)[a]	K (**12a/12b**)	Equilibrium time[b]
293	1.14	several days
313	4.33	50 h
328	4.91	8.5 h
343	4.29	4 h

[a] Equilibrium constants K are based on the integrals of the cyclopentadienyl groups in the ^{1}H NMR spectra. [b] Time required to reach equilibrium when dissolving **12** at 293 K and warming to the temperature cited.

A pathway for the interconversion between **12a** and **12b** is tentatively proposed (Scheme 7). Formally, the transformation involves the interchange of the orientation of H and Me_3Si in one of the two four-membered rings (shown for the left ring in Scheme 7). The process must be intramolecular as the reactive metalla-alkene units could not be liberated by coordination of magnesium bromide upon addition of dioxane. Furthermore, the position of the equilibrium is concentration independent; at 313 K, in a separate experiment with a diluted solution of the **12a/b** mixture, the same reaction rate and equilibrium constant as in the undiluted experiment were found. We propose that, in **12a** or **12b**, one of the carbon−magnesium bonds is cleaved such that the formal $Cp_2Zr-CHSiMe_3^-$ substructure can rotate around the Zr−C bond, followed by reclosure of the C−Mg bond; simultaneous cleavage of the Zr−Br bond, with formation of the more or less free metalla-alkene [$Cp_2Zr{=}CHSiMe_3$], can be excluded as it should lead to decomposition with formation of free $MgBr_2$ and dimerization of [$Cp_2Zr{=}CHSiMe_3$] to give **14** (Scheme 5).

The temperature dependence of the equilibrium between **12a** and **12b** was studied by ^{1}H NMR spectroscopy with a sample in a sealed NMR tube (Table 5); at higher temperatures, the equilibrium shifted in favor of **12a**. Consequently, we expected the highest **12a/b** ratio at 343 K, but this was not observed. It is not clear what caused this deviation as the compounds did not decompose; for several measurements of the same NMR sample at higher temperatures the **12a/b** ratio returned to the initially determined K of 1.14 at 20°C. In view of this anomaly, the interpretation of these results must remain speculative and we refrain from a quantitative analysis; however, some qualitative conclusions may be justified. Thus, **12b** appears to be enthalpically more stable than **12a**. This seemed surprising as, intuitively, one would assume that **12a** with its two bulky trimethylsilyl groups *trans* at the two four-membered rings will experience less steric hindrance than **12b**, where they are somewhat closer; however, inspection of models suggests that in both isomers the trimethylsilyl groups do not interfere directly with each other. Conversely, the trimethylsilyl groups of **12b** can adopt a favorable position between the bulky cyclopentadienyl groups with less distortion of the two four-membered rings, and less concomitant strain, than those of **12a**. In contrast, the reaction entropy appears to favor **12a**; given the close similarity of the two isomers, we have at present no satisfactory explanation for this effect.

Conclusion

In line with earlier results on the reduced reactivity of organomagnesium reagents that carry electropositive substituents at the organometallic carbon atom,[15,16] the 1,1-di-Grignard reagent $Me_3SiCH(MgBr)_2$ (**8**) reacts sluggishly with transition metal dihalides and, mostly, gave no well-defined products. An exception is the reaction of **8** with [Cp_2ZrCl_2] (1:1) which, in low yield, furnished the novel spiro-organomagnesium compound [$Cp_2ZrCHSiMe_3(\mu\text{-}Br)]_2Mg$ (**12**). Compound **12** is stable at room temperature and does not disproportionate on addition of dioxane. An X-ray crystal structure determination showed that, in the solid state, **12** is present as the C_2 symmetric stereoisomer **12a**; it is sterically very crowded due to the trimethylsilyl substituents. Partial metalla-alkene character is indicated by the short zirconium−carbon bonds, and agostic zirconium−hydrogen interactions by the short zirconium−hydrogen distances (Zr···H−C) and small $^1J_{C,H}$ coupling constants. In benzene solution, an equilibrium between **12a** and its C_1 symmetric stereoisomer **12b** was detected by ^{1}H and ^{13}C NMR spectroscopy.

Experimental Section

General Remarks: Experiments with **8** and **12** were performed using high-vacuum sealed glass apparatus.[26] Solvents were dried before use by distillation from a liquid Na−K alloy. For spectroscopy, the solvent was first removed from a sample by distillation with liquid nitrogen, followed by evacuation; subsequently, the residue was redissolved in a deuterated solvent in a high-vacuum system and, finally, the NMR tube was sealed. NMR spectra were measured with a Bruker WM 250 spectrometer. GCMS analysis was per-

formed on a Hewlett Packard 5890 GC/5970 MS combination with a 50 m Chrompack CP Sil 5 column.

2,2,6,6-Tetracyclopentadienyl-3,7-bis(trimethylsilyl)-1,5-dibroma-4-magnesa-2,6-dizirconaspiro[3.3]heptane (12): In a sealed glass vessel, **8**[15] (0.202 mmol) was dissolved in 2-methyltetrahydrofuran (10 mL). [Cp_2ZrCl_2] (59 mg, 0.202 mmol) was then added to this solution at −20 °C, resulting in a colorless solution. After 50 min stirring at −20 °C, the mixture was still colorless and homogeneous. The vessel was then warmed to +5 °C and, after 25 min, the mixture turned light yellow. Subsequently, the vessel was warmed and kept at room temperature for 4 h. The reaction mixture was yellow, and no precipitation was observed. After a further 17 h at room temperature, the solution became yellow-brownish. The solvent was then removed by distillation and pumping. The resultant residue was partly crystalline, partly oily. It was extracted with toluene to give a brownish solution, which was decanted from the precipitate of salts. Attempts to prepare crystals on cooling this solution (at −10 °C or −80 °C) failed. Toluene was removed by distillation into a vessel cooled by liquid nitrogen; a yellow oil was left in which crystals formed after several weeks. These were then washed with hexane; the light yellow hexane solution was decanted. The residue was made solvent free by distillation with liquid nitrogen and then toluene was added. Some precipitate (probably magnesium salts) formed, and the solution was decanted. After several further weeks at room temperature, a few pale yellow-orange crystals precipitated from this solution; they were used for X-ray crystal structure determination and for NMR measurements. The mother liquor, which contained mainly **12** (NMR analysis), was treated with dioxane. A small amount of a white precipitate ($MgBr_2$) formed, but NMR analysis of an aliquot revealed that no apparent change had taken place. **12a:** ^{1}H NMR (250 MHz, C_6D_6, ref.C_6D_5H δ = 7.17 ppm): δ = 7.43 (s, 2 H, methine), 6.09 (s, 10 H, Cp), 5.94 (s, 10 H, Cp), 0.43 (s, 18 H, Me) ppm. ^{13}C NMR (62.9 MHz, C_6D_6, ref.C_6D_6 δ = 128.0 ppm): δ = 153.3 (d, $^1J_{C,H}$ = 91.4 Hz, methine), 111.4 (dquint., $^1J_{C,H}$ = 172.5, $J_{C,H}$ = 6.9 Hz, Cp), 110.1 (dquint., $^1J_{C,H}$ = 173.1, $J_{C,H}$ = 6.8 Hz, Cp), 6.4 (q, $^1J_{C,H}$ = 117.2 Hz, Me) ppm. **12b:** ^{1}H NMR (250 MHz, C_6D_6, ref.C_6D_5H δ = 7.17 ppm): δ = 7.80 (s, 1 H, methine), 7.17 (s, 1 H, methine), 6.14 (s, 5 H, Cp), 6.04 (s, 5 H, Cp), 5.95 (s, 5 H, Cp), 5.94 (s, 5 H, Cp), 0.43 (s, 9 H, Me), 0.40 (s, 9 H, Me) ppm. ^{13}C NMR (62.9 MHz, C_6D_6, ref.C_6D_6 δ = 128.0 ppm): δ = 152.5 (d, $^1J_{C,H}$ = 88.5 Hz, methine), 145.6 (d, $^1J_{C,H}$ = 90.3 Hz, methine), 111.8 (dquint., $^1J_{C,H}$ = 172.7, $^1J_{C,H}$ = 6.7 Hz, Cp), 111.5 (dquint., $^1J_{C,H}$ = 173, $J_{C,H}$ = 7 Hz, Cp), 110.7 (dquint., $^1J_{C,H}$ = 173.2, $J_{C,H}$ = 6.8 Hz, Cp), 109.9 (dquint., $^1J_{C,H}$ = 173.1, $J_{C,H}$ = 6.7 Hz, Cp), 6.9 (q, $^1J_{C,H}$ = 117.2 Hz, Me), 6.2 (q, $^1J_{C,H}$ = 117.2 Hz, Me) ppm.

X-ray Crystal Structure Determination of 12: $C_{28}H_{40}Br_2MgSi_2Zr_2$. M = 799.35, pale orange crystal, 0.21 × 0.23 × 0.40, monoclinic, space group $P21/c$ (no. 14) with a = 14.7539(5), b = 12.3679(4), c = 17.8513(7) Å; β = 93.83(3)°, V = 3250.1(2) Å^3, Z = 4, $\rho_{calcd.}$ = 1.633 g·cm^{-3}, $F(000)$ = 1592, μ(Mo-K_α) = 3.17 mm^{-1}. Of the 9029 reflections measured on an Enraf−Nonius CAD4-T diffractometer, on a rotating anode [λ(Mo-K_α) = 0.71073 Å, T = 295 K, $\theta_{max.}$ = 27.5°], 7430 were unique (R_{int} = 0.029); 4477 reflections with $I > 2.5\sigma(I)$ were used in the structure solution and refinement. Application of empirical and analytical absorption correction algorithms on the measured data had no significant effect. A final model without absorption correction was therefore preferred. The structure was solved with Patterson methods (SHELXS-86[27]); 317 parameters were refined with SHELX-76,[28] including anisotropic displacement parameters for all non-hydrogen atoms. Hydrogen atoms were placed at calculated positions, riding on their carrier atoms, with the exception of hydrogen atoms bonded to C11 and C25 (the carbon atoms bonded to Mg, Br, and Zr). The coordinates of these hydrogen atoms were allowed to refine, albeit that the C−H bond length was constrained to the ideal value of 0.98 Å. Final figures of merit are R = 0.054, R_w = 0.073, S = 2.94. Residual density was in the range −1.34, 1.13 e·Å^3. CCDC-222722 contains the supplementary crystallographic data for this paper. These data can be obtained free of charge at www.ccdc.cam.ac.uk/conts/retrieving.html [or from the Cambridge Crystallographic Data Centre, 12 Union Road, Cambridge CB2 1EZ, UK; Fax: (internat.) +44-1223-336-033; E-mail: deposit@ccdc.cam.ac.uk].

Acknowledgments

This work was supported in part (ALS) by the Council for the Chemical Sciences of the Netherlands Organization for Scientific Research (CW-NWO).

[1] F. N. Tebbe, G. W. Parshall, G. S. Reddy, *J. Am. Chem. Soc.* **1978**, *100*, 3611−3613.
[2] S. H. Pine, R. Zahler, D. A. Evans, R. H. Grubbs, *J. Am. Chem. Soc.* **1980**, *102*, 3270−3272.
[3] J. W. Bruin, G. Schat, O. S. Akkerman, F. Bickelhaupt, *Tetrahedron Lett.* **1983**, *24*, 3935−3936.
[4] B. J. J. van de Heisteeg, G. Schat, O. S. Akkerman, F. Bickelhaupt, *Tetrahedron Lett.* **1987**, *28*, 6493−6496.
[5] G. Emschwiller, *C. R. Acad. Sci. Paris* **1926**, *183*, 665.
[6] F. Bertini, P. Grasselli, G. Zubiani, G. Cainelli, *Tetrahedron* **1970**, *26*, 1281, and ref. cited.
[7] J. W. Bruin, G. Schat, O. S. Akkerman, F. Bickelhaupt, *J. Organomet. Chem.* **1985**, *288*, 13−25.
[8] B. J. J. van de Heisteeg, G. Schat, O. S. Akkerman, F. Bickelhaupt, *J. Organomet. Chem.* **1986**, *308*, 1−10.
[9] B. J. J. van de Heisteeg, G. Schat, O. S. Akkerman, F. Bickelhaupt, in *Organometallic Syntheses* (Eds.: R. B. King, J. J. Eisch), Elsevier, Amsterdam, **1988**, Vol. 4, 389−391.
[10] F. Bickelhaupt, *Angew. Chem.* **1987**, *99*, 1020−1035; *Angew. Chem. Int. Ed. Engl.* **1987**, *26*, 990.
[11] F. Bickelhaupt, *J. Organomet. Chem.* **1994**, *475*, 1−14.
[12] K. C. Kennon, G. R. Krow, in *Handbook of Grignard Reagent*s (Eds.: G. S. Silverman, P. E. Rakita), Marcel Dekker, New York, **1996**, 497−526.
[13] F. Bickelhaupt, in *Grignard Reagents, New Developments* (Ed.: H. G. Richey), Wiley, Chichester, **2000**, 367−393.
[14] B. J. J. van de Heisteeg, G. Schat, O. S. Akkerman, F. Bickelhaupt, *J. Organomet. Chem.* **1986**, *108*, C25−C28.
[15] B. J. J. van de Heisteeg, G. Schat, M. A. G. M. Tinga, O. S. Akkerman, F. Bickelhaupt, *Tetrahedron Lett.* **1986**, *27*, 6123−6324.
[16] M. Hogenbirk, G. Schat, M. A. G. M. Tinga, O. S. Akkerman, F. Bickelhaupt, W. J. J. Smeets, A. L. Spek, *J. Am. Chem. Soc.* **1992**, *114*, 6195−6198.
[17] H. L. Uhm, in *Handbook of Grignard Reagent*s (Eds.: G. S. Silverman, P. E. Rakita), Marcel Dekker, New York, **1996**, 117−144.
[18] F. Bickelhaupt in *Grignard Reagents, New Developments* (Ed.: H. G. Richey), Wiley, Chichester, **2000**, 298−328.
[19] U. Klabunde, F. N. Tebbe, G. W. Parshall, R. L. Harlow, *J. Mol. Cat.* **1980**, *8*, 37−51.
[20] W. E. Hunter, D. C. Hrncir, R. Vann Bynum, R. A. Penttila, J. L. Atwood, *Organometallics* **1983**, *2*, 750−755.
[21] J. Jeffery, M. F. Lappert, N. T. Luong-Thi, J. L. Atwood, W. E. Hunter, *J. Chem. Soc., Chem. Commun.* **1978**, 1081−1083.

[22] G. Erker, R. Zwettler, C. Krüger, R. Noe, S. Werner, *J. Am. Chem. Soc.* **1990**, *112*, 9620−9621.
[23] I. Hyla-Kryspin, R. Gleiter, C. Krüger, R. Zwettler, G. Erker, *Organometallics* **1990**, *9*, 517−523.
[24] M. Brookhart, M. L. H. Green, *J. Organomet. Chem.* **1983**, *285*, C5−C8.
[25] M. Brookhart, M. L. H. Green, L.-L. Wong, *Prog. Inorg. Chem.* **1988**, *36*, 1−124.
[26] A. D. Vreugdenhil, C. Blomberg, *Recl. Trav. Chim. Pays Bas* **1963**, *83*, 453−460.
[27] G. M. Sheldrick, *SHELXS-86* Program for crystal structure determination, University of Göttingen, Germany, **1986**.
[28] G. M. Sheldrick, *SHELX-76* Program for crystal structure determination and refinement, University of Göttingen, Germany, **1976**.
[29] A. L. Spek, PLATON, A multi-purpose crystallographic tool, Utrecht University, The Netherlands, **2003**; Internet: http://www.cryst.chem.uu.nl/platon/

Received November 6, 2003
Early View Article
Published Online April 1, 2004

